ELSEVIER

Journal of Fluorine Chemistry 83 (1997) 41–45

JOURNAL OF FLUORINE CHEMISTRY

The effect of Lewis acid catalysis on the decomposition of CF_3OCF_3 to COF_2 and CF_4

J. Pacansky, R.J. Waltman

IBM Almaden Research Center, 650 Harry Road, San Jose, CA 95120-6099, USA

Received 25 July 1996; accepted 19 November 1996

Abstract

The CF_3OCF_3 and AlF_3 Lewis acid interaction is investigated by ab initio theory to explain the catalytically enhanced degradation of polyperfluorinated ether lubricants. Thus, an understanding of the Lewis acid interaction in these materials is gained by investigating the optimized geometries of CF_3OCF_3 in the presence and absence of AlF_3. The computed bond parameters and partial atomic charges identify a strong interaction between the aluminum substrate and the CF_3OCF_3 ether oxygen atom. A transition state that connects the reactant CF_3OCF_3 and products COF_2 and CF_4 is identified. The effect of the Lewis acid interaction on the transition state geometry is analyzed. A significant reduction in the activation energy to the transition state via the Lewis acid interaction is computed, providing a quantitative understanding for catalytically induced degradation in these materials. © 1997 Elsevier Science S.A.

Keywords: Decomposition; Perfluorodimethyl ethyl; Catalysis

1. Introduction

In a previous report, the decomposition of polyperfluorinated ethers was investigated by computing the reaction coordinate for the model system, perfluorodimethyl ether, CF_3OCF_3 [1]. CF_3OCF_3, like the perfluorinated ether polymers, produces COF_2 and CF_4 products upon degradation [2]. The decomposition reaction was computed to be exothermic at the higher levels of theory which included correlated wavefunctions. However, the activation energy leading to products was relatively high, of the order of 100 kcal mol^{-1} depending upon the level of theory employed. Consistently, the reaction path that provided the lowest activation energy involved a "cyclic" transition state which connected the reactant CF_3OCF_3 to products COF_2 and CF_4, compared with a direct C–O bond scission to produce $CF_3O^{\cdot}$ and $CF_3^{\cdot}$ radicals followed by a disproportionation reaction of the radicals.

While the temperatures required to cause the intrinsic decomposition of polyperfluorinated ethers is high, $\simeq$350 °C, they readily decompose at much lower temperatures, e.g. $\simeq$150 °C, on metal surfaces [3]. XPS studies have revealed that the metal surface is converted to a metal halide, creating the possibility for a Lewis acid interaction with the perfluorinated ether [4]. Hence, a realistic extension of these studies is to investigate the same reaction path with the addition of the metal–CF_3OCF_3 interaction. These results indicate a significant catalytic effect by AlF_3, which reduces the activation energy for decomposition of CF_3OCF_3 to COF_2 and CF_4 from $\simeq$100 to 50 kcal mol^{-1}. The details of the catalytic effect are disclosed.

2. Computational method

Ab initio calculations were performed using the Mulliken computer code [5], using IBM RISC 6000 computers. Hartree–Fock (HF) calculations were performed using the 6-31G* basis set [6]. Harmonic vibrational frequencies were calculated by differentiation of the energy gradient at the optimized geometries. No imaginary frequencies were computed at minima; one imaginary frequency at the maximum (transition state).

3. Results and discussion

The optimized geometries for perfluorodimethyl ether, CF_3OCF_3, hereafter referred to as PFDME, with and without the AlF_3 interaction are presented in Fig. 1 for direct comparison. The optimized parameters are summarized in Table 1. AlF_3 is used here as a model for the Lewis acid,

PII S0022-1139(96)03563-4

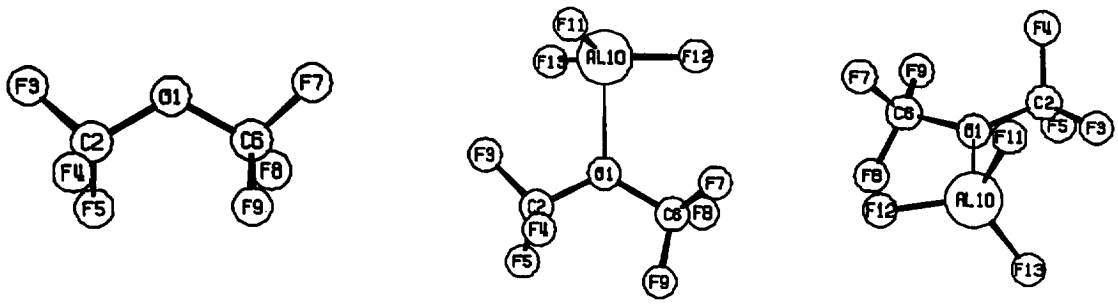

Fig. 1. The optimized geometries for PFDME (left) and two perspectives for PFDME–AlF_3 (middle, right).

Table 1
HF/6-31G* optimized bond distances (Å), angles (deg) and dihedrals (deg) [a]

Parameters	PFDME	PFDME–AlF_3	TS	TS–AlF_3
O1–C2	1.356	1.393	1.230	1.282
O1–C6	1.356	1.402	2.402	2.759
O1–Al10	–	2.153	–	1.830
C2–F3	1.301	1.294	1.331	1.314
C2–F4	1.308	1.297	1.331	1.317
C2–F5	1.310	1.297	1.468	1.380
F5–C6	2.695	2.856	2.200	2.501
C6–F7	1.301	1.292	1.227	1.212
C6–F8	1.308	1.292	1.238	1.228
C6–F9	1.310	1.301	1.225	1.213
Al10–F11	–	1.631	–	1.642
Al10–F12	–	1.633	–	1.676
Al10–F13	–	1.631	–	1.658
O1–C2–F3	107.09	105.98	118.58	115.62
O1–C2–F4	111.25	110.34	118.61	113.70
O1–C2–F5	111.82	110.34	107.70	108.84
O1–C6–F7	107.09	108.43	77.70	81.66
O1–C6–F8	111.25	108.22	135.30	123.69
O1–C6–F9	111.82	110.07	81.99	–
O1–Al10–F11	–	97.82	–	111.93
O1–Al10=F12	–	93.27	–	97.22
O1–Al10–F13	–	98.29	–	103.80
C2–O1–C6	121.30	121.27	96.95	96.57
C2–O1–Al10	–	118.68	–	133.20
C2–F5–C6	–	–	98.92	106.04
F5–C6–F7	–	–	115.45	88.37
F5–C6–F8	–	–	80.59	78.49
F5–C6–F9	–	–	96.20	110.15
C6–O1–Al10	–	119.97	–	97.21
F7–C6–F8	108.96	110.64	115.57	118.75
F7–C6–F9	109.36	109.69	121.46	122.64
F11–Al10–F12	–	118.39	–	115.79
F11–Al10–F13	–	119.39	–	117.42
F12–Al10–F13	–	118.45	–	108.22
O1–C2–F3–F4	120.43	119.34	136.06	128.38
C2–O1–C6–F9	−43.47	2.69	–	–
C2–F5–C6–F7	–	–	−53.68	−83.12
F5–C2–O1–C6	−43.47	−61.99	0.85	4.85
F5–C2–O1–Al10	–	121.25	–	102.09
C6–O1–C2–F3	−163.25	178.92	–	−122.71
F7–C6–O1–C2	−163.25	−117.31	–	98.25
F12–Al10–O1–C2	–	178.28	–	−144.66
Energy (hartee)	−747.26551633	−1287.73170493	−747.09727998	−1287.64071436

[a] AlF_3 optimized geometry: Al–F, 1.620 Å; F–Al–F, 120.0°; total energy, −540.45045157 hartrees.

Table 2
HF/6-31G* computed bond orders

Parameters	PFDME	PFDME–AlF_3	TS	TS–AlF_3
O1–C2	0.902	0.757	1.503	1.138
O1–C6	0.902	0.731	0.140	0.342
O1–Al10	–	0.138	–	0.442
C2–F3	0.996	0.980	0.917	0.941
C2–F4	0.974	0.978	0.917	0.956
C2–F5	0.957	0.980	0.596	0.766
F5–C6	0.016	0.009	0.161	0.069
C6–F7	0.996	1.001	1.219	1.259
C6–F8	0.974	1.002	1.181	1.215
C6–F9	0.957	0.975	1.206	1.266
Al10–F11	–	0.772	–	0.758
Al10–F12	–	0.751	–	0.649
Al10–F13	–	0.774	–	0.711

because it has comparatively few electrons and is a closed shell. The actual surface may be ionic although possibly more coordinatively unsaturated than the bulk.

The most notable changes that occur in the optimized geometry of PFDME–AlF_3 are an increase in the C–O bond length by $\simeq 0.04$ Å, and rotation of the CF_3– end groups such that a C–F bond in each end group closest to the C–O–C backbone is very nearly coplanar to the C–O–C backbone, compared with the normal $\approx 17°$ rotation out of the C–O–C plane in PFDME. Thus, the C6–O1–C2–F3 and F7–C6–O1–C2 dihedral angles are 179° and 3°, respectively, in PFDME–AlF_3, compared with $-163.3°$ for both dihedral angles in PFDME. The rotation of the CF_3– end groups in PFDME–AlF_3 is necessary to spatially accommodate the fluorine atoms bonded to aluminum, F11, F12, and F13, so that they may be at their optimum van der Waals distances from the CF_3OCF_3 skeleton, i.e., F3 with F11 and F13, respectively, and F12 with F7 and F8, respectively, all distances near 2.8–2.9 Å. This arrangement also optimizes the Al10–O1 distance at 2.153 Å, $\simeq 0.25$ Å longer than normal Al–O bonding distances. However, this distance is also considerably shorter than the typical $\simeq 3$ Å found in Al···O non-bond distances. Hence, the Lewis acid interaction is apparently quite significant. The computed bond orders in Table 2 provide further insight into the Lewis acid interaction. In particular, the O1–Al10 bond order of 0.138, while small, is indicative that the two atoms have a mutual attraction. The small magnitude of the bond order suggests that the interaction is not strongly covalent; hence, it must largely be electrostatic, which is the norm for Lewis acid interactions.

Population analyses indicate that when CF_3OCF_3 and AlF_3 are infinitely apart, the highest occupied molecular orbital (HOMO) for CF_3OCF_3 is dominated by the lone pair of electrons on the ether oxygen atom which contributes as a donor. For AlF_3, the empty LUMO (lowest unoccupied molecular orbital) on aluminum serves as a good acceptor. Thus, the oxygen–aluminum provides an excellent Lewis acid/base system.

The computed partial atomic charges, summarized in Table 3, indicate that the C–O bonds in PFDME are quite polar, the oxygen atom O1 having an excess negative charge of $-0.44\ e^-$ while the carbon atoms C2 and C6 are excess positive by $+0.82\ e^-$. Hence, the C–O bond is susceptible to Lewis acid attack. For example, the Al atom in AlF_3 is positive by $+1.9\ e^-$ and thus, interacts strongly with O1 in PFDME. The interaction results in the structure PFDME–

Table 3
The partial atomic charges computed at the HF/6-31G* optimized geometries, using an electrostatic potential fit to the molecules

Atom	PFDME	PFDME–AlF_3	TS	TS–AlF_3	AlF_3
O1	−0.439	−0.545	−0.793	−0.759	
C2	+0.822	+0.851	+0.982	+0.922	
F3	−0.191	−0.175	−0.286	−0.229	
F4	−0.204	−0.177	−0.287	−0.241	
F5	−0.208	−0.177	−0.394	−0.337	
C6	+0.822	+0.826	+0.903	+1.055	
F7	−0.191	−0.165	−0.028	−0.044	
F8	−0.204	−0.165	−0.065	−0.073	
F9	−0.208	−0.179	−0.033	−0.038	
Al10		+1.530		+1.480	+1.866
F11		−0.542		−0.556	−0.622
F12		−0.542		−0.596	−0.622
F13		−0.542		−0.583	−0.622

AlF_3, which polarizes the C–O bond still further by increasing the excess negative charge on O1 from $-0.44\ e^-$ in PFDME to $-0.55\ e^-$ in PFDME–AlF_3. The strong Al10···O1 interaction in PFDME–ALF_3 reduces the excess positive charge in Al10 from $+1.9\ e^-$ in AlF_3 to $+1.5\ e^-$ in PFDME–AlF_3.

Several orientations of the optimized transition state structures, TS and TS–AlF_3, are presented in Fig. 2. The TS structure is presented here for direct comparison with the TS–AlF_3 geometry and is discussed only to the extent necessary to delineate the geometric changes caused by the Lewis acid interaction. In both cases, the O1–C2–F5–C6 cluster forms a "cyclic" structure that is coplanar, with the dihedral angle being 0.85° and 4.85° for TS and TS–AlF_3, respectively. The side by side comparison clearly shows that the gross structural features of both transition state geometries are similar. There are, however, some noteworthy differences. First, the C2–O1 bond length in TS–AlF_3, 1.282 Å, is considerably longer than the 1.230 computed for TS. In the TS–AlF_3 structure, the O1–C6 and F5–C6 atom distances are 2.759 Å and 2.501 Å, respectively, compared with 2.402 Å and 2.200 Å, respectively, and hence are significantly longer. In addition, the C2–F5 atom distance in TS–AlF_3, computed at 1.380 Å, is 0.088 Å shorter than in TS. As regards the Lewis acid interaction, the Al10–O1 distance is now considerably shortened compared with PFDME–AlF_3, to 1.83 Å, consistent with distances typically found in formal Al–O bonds.

The computed bond orders, summarized in Table 2, indicate a 220% increase in the O1–Al10 bond order in TS–AlF_3 compared with PFDME–AlF_3, from 0.138 to 0.442, respectively. A comparison of the O1–C6 bond orders in TS and TS–AlF_3 indicates that, despite the longer O1–C6 bond distance in TS–AlF_3, the corresponding bond order is in fact larger by 144%. The C2–F5 bond order in TS–AlF_3, 0.766, is 28% larger than in TS, while the F5–C6 bond order in TS–AlF_3, 0.069, is 56% smaller than in TS. The C2–O1 bond order, 1.503 in TS, is significantly smaller in TS–AlF_3, 1.138. These data indicate the following: (1) in the TS geometry, the O1, C2, F3, and F4 cluster has considerable COF_2 character and hence the transition state is well on its way to the COF_2 and CF_4 products; (2) in the TS–AlF_3 geometry, the O1, C2, F3, and F4 cluster maintains greater ether character than the transition structure without the AlF_3 interaction, TS in Fig. 2, even though some progress towards a more COF_2-like local structure for the O1, C2, F3, and F4 cluster has been made. Hence, the C2–F5 and F5–O6 bonds exhibit larger and smaller bond orders, respectively. One interpretation of the longer O1–C6 bond distance in TS–AlF_3 might have been that the scission process to products is more complete at the transition structure; however, the bond order data merely reflects the more asynchronous nature of the transition state structure at the TS geometry compared with TS–AlF_3 geometry.

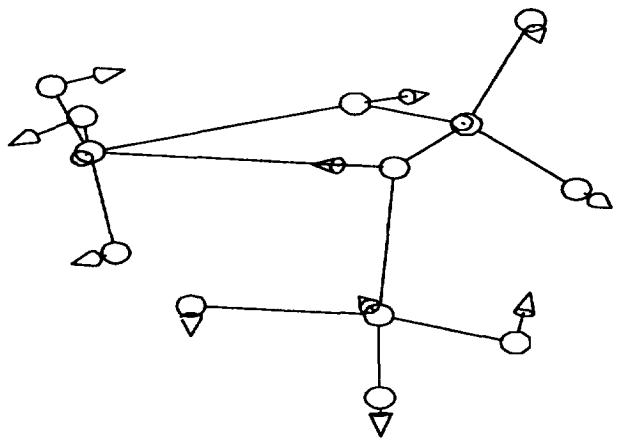

Fig. 3. The normal mode vector for the imaginary frequency, $-116\ cm^{-1}$, found for TS–AlF_3. The orientation of the molecule is the same as the middle picture in Fig. 2.

The computed partial atomic charges for TS–AlF_3 are summarized in Table 3. It appears that the partial atomic charges computed in TS–AlF_3 are slightly smaller in magnitude than the corresponding atomic charges in TS, for O1, C2, F3, F4, F5, and Al10 atoms. Hence, the polarity of the bonds in TS–AlF_3 are somewhat less than found for TS. These results corroborate the interpretation that the transition geometry in TS–AlF_3 retains more ether character than TS, and that the transition state structure is stabilized by the presence of the AlF_3.

Finally, to complete the geometry characterization, we report a computed imaginary frequency of $-116\ cm^{-1}$ for TS–AlF_3. As shown in Fig. 3, the amplitude of the normal mode vectors are largest for the O1 and F5 atoms connected to C2, thus the transition structure appears to connect the reactant CF_3OCF_3 to products COF_2 and CF_4.

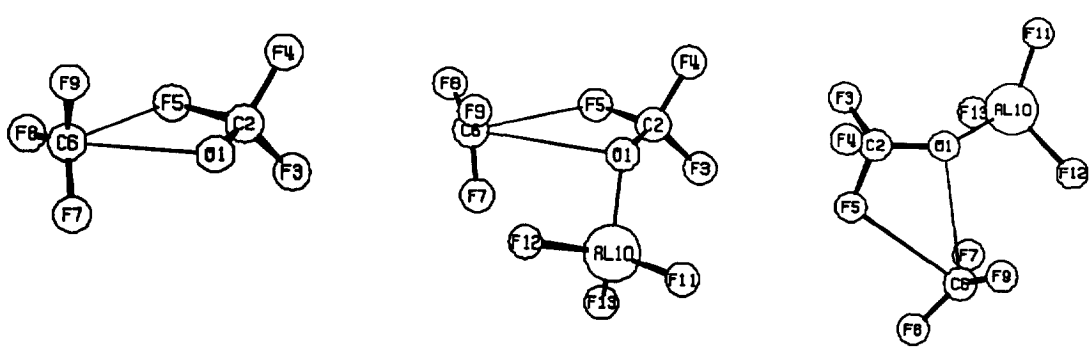

Fig. 2. The optimized geometries for the transition states TS (left) and two perspectives for TS–AlF_3 (middle, right).

Table 4
The reaction coordinates, ΔE, HF/6-31G*, corrected for zero-point energies, for the two reaction paths. All energies relative to reactant

Structure	With AlF_3	Without AlF_3
Reactant:		
CF_3OCF_3 ($\pm AlF_3$)	0	0
Metal–ether:		
$CF_3OCF_3\cdots AlF_3$, Fig. 1 left)	−9.06	
Intermediate:		
TS (Fig. 1, right, for $+AlF_3$)	47.13	103.38
Product:		
COF_2+CF_4 ($\pm AlF_3$)	0.97	0.97

3.1. The reaction coordinate

The energetics for the decomposition of CF_3OCF_3 to products COF_2 and CF_4, via the cyclic transition state, and in the presence and absence of AlF_3, are summarized in Table 4. The activation energy without the AlF_3 catalyst is 103 kcal-mol^{-1}. In the presence of the AlF_3 catalyst, Table 4 reveals a rather dramatic decrease in the activation energy to 47 kcal-mol^{-1}. Hence, the catalyst alters the reaction path although it does not change the initial and final states, i.e., ΔE remains the same. We also note a 9 kcal mol^{-1} lowering in energy in the PFDME–AlF_3 complex which we interpret as an interaction or binding energy between CF_3OCF_3 and AlF_3.

4. Concluding remarks

Lewis acid catalysis significantly enhances the thermally induced degradation of polyperfluorinated ether lubricants. Using CF_3OCF_3 and AlF_3, we have characterized one model for the Lewis acid interaction and the origin for the catalytic degradation. The optimized geometries identify a strong electrostatic interaction between the aluminum substrate and the CF_3OCF_3 ether oxygen atom which stabilizes the transition structure that occurs between reactant and product (COF_2, CF_4). At the transition geometry, the Al–O interaction develops some covalent character and the transition state is less asynchronous than without the catalyst. The effect of the catalyst is to reduce the activation energy for decomposition from 103 to 47 kcal mol^{-1}. This provides a fundamental understanding on why catalytic surfaces must be avoided to ensure the integrity of polyperfluorinated ether lubricants.

References

[1] J. Pacansky, R.J. Waltman, J. Fluorine Chem., in press.
[2] J. Pacansky, R.J. Waltman, manuscript in preparation, 1996.
[3] P.H. Kasai, P. Wheeler, Appl. Surf. Sci. 52 (1991) 91.
[4] S. Mori, W. Morales, Wear 132 (1989) 111.
[5] H. Horn, B.H. Lengsfield, J.E. Rice, A.D. McLean, J.T. Carter, E.S. Replogle, L.A. Barnes, S.A. Maluendes, G.C. Lie, M. Gutowski, W.E. Rudge, S.P.A. Sauer, R. Lindh, K. Andersson, T.S. Chevalier, P.-O. Widmark, D. Bouzida, G. Pacansky, K. Singh, C.J. Gillan, P. Carnevali, W.C. Swope,, B. Liu, Mulliken 2.0, Almaden Research Center, IBM Research Division, 6500 Harry Road, San Jose, CA 95120-6099.
[6] K. Raghavachari, J.A. Pople, Int. J. Quant. Chem. 20 (1981) 1067.